DOI 10.1007/s10593-021-02904-8

Chemistry of Heterocyclic Compounds **2021**, *57*(3), 274–283

Electrocatalytic tandem assembly of aldehydes with 2-thiobarbituric acid into 5,5'-(arylmethylene)bis(1,3-diethyl-2-thiobarbituric acids) and evaluation of their interaction with catalases

Michail N. Elinson[1], Anatoly N. Vereshchagin[1], Yuliya E. Ryzhkova[1], Kirill A. Karpenko[1], Fedor V. Ryzhkov[1]*, Mikhail P. Egorov[1]

[1] *N. D. Zelinsky Institute of Organic Chemistry, Russian Academy of Sciences, 47 Leninsky Ave., Moscow 119991, Russia; e-mail: ryzhkov.fe@ya.ru*

Published in Khimiya Geterotsiklicheskikh Soedinenii, 2021, *57*(3), 274–283

Submitted October 7, 2020
Accepted after revision December 12, 2020

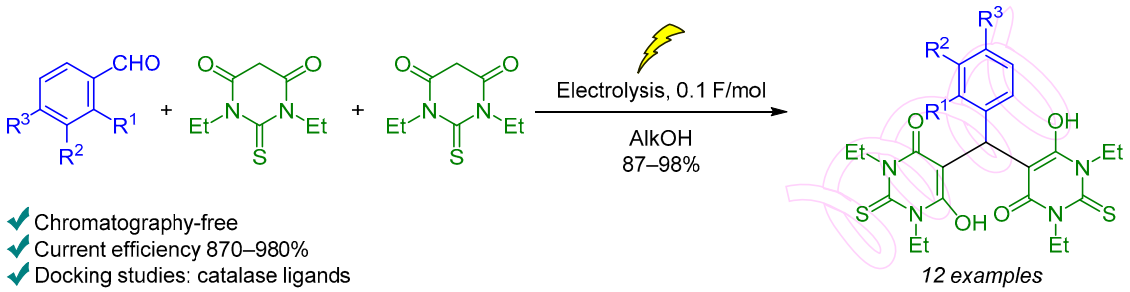

Electrocatalytic transformation of aldehydes with two equivalents of 1,3-diethyl-2-thiobarbituric acid has been carried out in alcohols in an undivided cell in the presence of sodium halides with the selective formation of the substituted 5,5'-(arylmethylene)bis(1,3-diethyl-2-thiobarbituric acids) in 87–98% yields and with 870–980% current efficiency. This new one-pot electrochemically induced tandem Knoevenagel–Michael process is a simple and efficient approach to substituted 5,5'-(arylmethylene)bis(1,3-diethyl-2-thiobarbituric acids) containing two 1,3-diethyl-2-thiobarbituric acid fragments separated by *C*-aryl-substituted spacer, which are promising compounds for different biomedical applications, including anticonvulsant, antiAIDS agents and anti-inflammatory remedies. Theoretical studies were carried out to investigate the interaction of the synthesized compounds with beef and human catalases.

Keywords: aldehydes, 5,5'-(arylmethylene)bis(1,3-diethyl-2-thiobarbituric acids), 1,3-diethyl-2-thiobarbituric acid, docking studies, electrocatalysis, electroorganic chemistry.

The continuously growing interest in convenient and green reaction techniques encourages organic chemists to elaborate new synthetic methodologies.[1] Tandem reaction is the combination of two or more reactions, which take place in a specific order.[2] These reactions are also one-pot processes and, hence, such a method of synthesis is a very powerful way to the rapid and efficient construction of complex organic molecules.[2] These reactions adhere to green chemistry principles, as the stages of isolation and purification of intermediates are omitted, which leads to diminished pollution of the environment. In addition to the intrinsic atom economy and selectivity, the tandem reaction strategy offers significant advantages over conventional linear-type synthesis due to its flexible and convergent nature.[3]

Tandem Knoevenagel–Michael process is a special case of both cascade and multicomponent reactions, in which Knoevenagel condensation is directly followed by Michael addition.[2] This complex one-pot transformation is an efficient method of organic synthesis,[2] and in the last decade new types and applications of this methodology are being intensively studied.[4–13]

The electroorganic synthesis is also attractive method, especially taking into consideration ecological demands of modern green chemistry.[14,15] Although application of electrolytic methods in organic synthesis is often limited with equipment complicacy and long reaction time, the utilization of electrogenerated base has become popular. An electrogenerated base is an anion that is formed *in situ* directly on a cathode. Electrogenerated base may be used as a homogeneous catalyst under reaction conditions instead of classic bases, such as alkaline or amine. Due to its nature, it allows to regulate formation of the catalyst during electrolysis and reduce the reaction of waste. Electroorganic reactions of such type proceed smoothly with easy workup and do not require the use of harsh conditions and expensive reagents.[16–21]

During our research in the field of electroorganic synthesis, we have found the electrochemical catalytic process,

induced by an electrogenerated base in an electrolyzer without diaphragm.[22] We have already used this electrolytic method for the synthesis of biologically active 2-amino-4*H*-chromenes.[23–25] This convenient and efficient electrocatalytic procedure utilizes cheap undivided cell. It is useful also for the large-scale synthesis thanks to the use of catalytic chain reaction and the application of inexpensive and environmentally clean electricity instead of chemical reagent. This catalytic methodology is very important for the organic synthesis, as it combines the efficiency of one-pot methods with the green chemistry advantages of electrolytic processes.[26, 27]

Heterocycles are the key structural compounds in medicinal chemistry, as they are found in many biologically important molecules such as enzyme, vitamins, natural products, and pharmacologically active compounds with antifungal, anti-inflammatory, antibacterial, antioxidant, anticonvulsant, anti-allergic, antiHIV, and anticancer activity.[28] Among the nitrogen-containing heterocycles, barbituric acid represents a type of a privileged medicinal scaffold.[29] Its 5-substituted derivatives are known as barbiturates. Many barbiturates are drugs that act on the central nervous system.[30] The current interest in barbiturates also arises from their pharmacological potential as antiAIDS[31] and anticancer agents.[32,33]

At the same time, the thiobarbituric acid derivatives also showed a broad range of pharmacological action, including diaminopimelate aminotransferase and tyrosinase inhibiting,[34] antituberculosis,[35] and anticancer in combination with anti-inflammatory activities.[36,37] Moreover, thiobarbituric acid was used in preparation of compounds, which possess quadratic non-linear optical (NLO) properties for optoelectronic and photonic technologies.[38]

Herein, we have attempted to connect two pharmacologycally active 1,3-diethyl-2-thiobarbituric moieties by a *C*-aryl-substituted spacer, presuming that introduction of two units of this medicinally privileged scaffold in one molecule could enhance pharmacological activity. We have already implemented some electrochemically induced multicomponent transformations of carbonyl compounds and different C–H acids.[39–44] In continuation of our study, now we report the data on the new selective and efficient electrocatalytic cascade assembly of aldehydes and two molecules of 1,3-diethyl-2-thiobarbituric acid in electrochemically induced tandem Knoevenagel–Michael reaction.

The electrolytic chain strategy is the simple and very efficient way to "ideal synthesis".[45] On this route, cascade reactions have sufficient overlap with PASE (Pot, Atom, and Step Economy) methodology.[46,47] PASE syntheses presuppose pot and step economy, but also introduce atom economy (with the aim that the most atoms of the starting compounds become part of the final product). In the case of electrocatalytic reactions, such process is also energy-economic due to high current efficiency (>100%).[48]

At the beginning of our investigation, to evaluate the synthetic potential of the electrocatalytic procedure and optimize the electrolysis conditions, the electrocatalytic cascade assembly of benzaldehyde **1a** with 2 equiv of 1,3-diethyl-2-thiobarbituric acid (**2**) was carefully studied under conditions of electrolysis in alcohols in an undivided cell (Table 1).

Data in Table 1 indicate, that the current density 5 mA/cm^2 (*I* 25 mA, *n*-PrOH as a solvent, NaBr as electrolyte) and the temperature near to the boiling point of *n*-PrOH were the optimal conditions for the electrochemically induced chain process and allowed for the highest isolated yield of

Table 1. Electrocatalytic coupling of benzaldehyde **1a** with 2 equiv of 1,3-diethyl-2-thiobarbituric acid (**2**)*

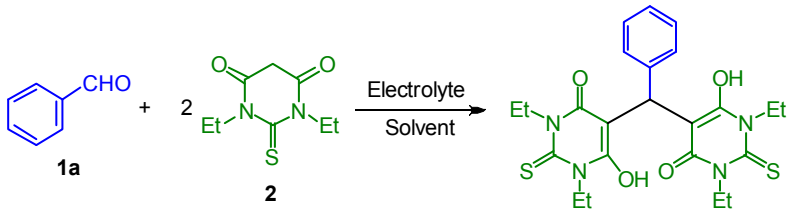

Entry	Solvent	Electrolyte	Temperature, °C	*I*, mA	Current density, mA/cm^2	Time, min	Electricity passed, *F*/mol	Yield, % (CE, %)**
1	MeOH	NaBr	25	25	5	32	0.1	12*** (120)
2	MeOH	NaBr	65	25	5	32	0.1	75 (750)
3	EtOH	NaBr	78	25	5	32	0.1	85 (850)
4	*n*-PrOH	NaBr	97	25	5	32	0.1	93 (930)
5	EtOH	NaBr	78	25	5	64	0.2	88 (440)
6	*n*-PrOH	NaBr	78	25	5	64	0.2	91 (455)
7	*n*-PrOH	NaBr	78	50	10	16	0.1	80 (800)
8	*n*-PrOH	NaBr	78	10	2	80	0.1	87 (870)
9	*n*-PrOH	NaI	78	25	5	32	0.1	89 (890)
10	*n*-PrOH	KBr	78	25	5	32	0.1	87 (870)

* Reaction conditions: benzaldehyde **1a** (5 mmol), 1,3-diethyl-2-thiobarbituric acid (**2**) (10 mmol), NaBr (1 mmol) as electrolyte, solvent (20 ml), iron cathode (5 cm^2), graphite anode (5 cm^2), undivided cell, electrode surface 5 cm^2.
** Current efficiency CE = $m \cdot F/(M_r \cdot I \cdot t) \cdot 100\%$, where m – the real obtained mass of compound; F – Faraday constant, $9.649 \cdot 10^4$ s·A/mol; M_r – molar mass of the product; I – electric current, A; t – reaction time, s.
*** ^{1}H NMR data.

Scheme 1. Electrocatalytic assembly of compounds **3a–l** (yields given in parentheses and current efficiency in brackets)

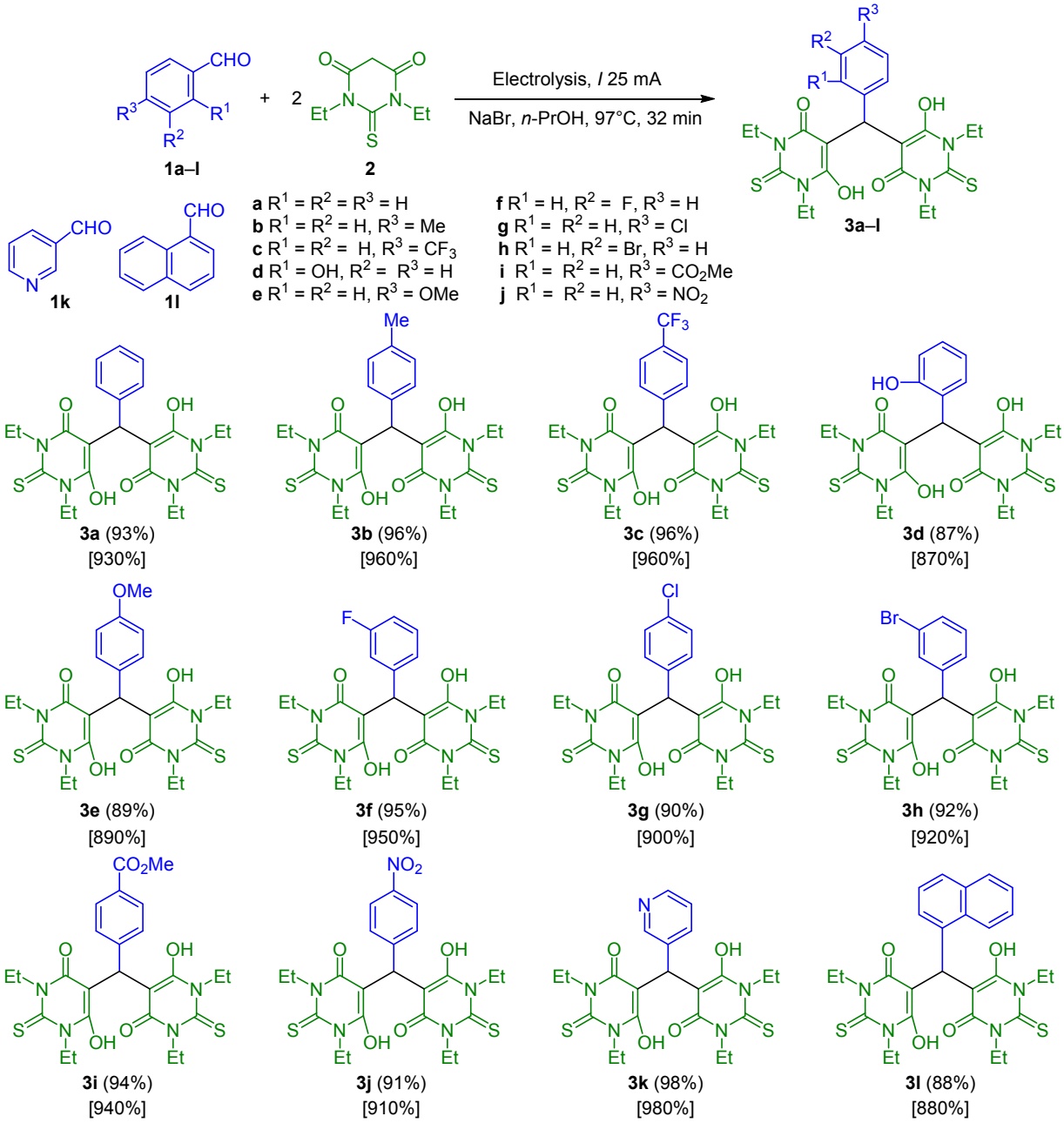

5,5'-(arylmethylene)bis(1,3-diethyl-2-thiobarbituric acid) (**3a**) (entry 4). When the current density 10 mA/cm^2 was used, both decrease of the substance yields and current efficiency have been observed (Table 1, entry 7). The current density 2 mA/cm^2 resulted in diminution of the substance yields and current efficiency (entry 8) as well. In the last case, this could be a result of inefficient induction of the electrolytic chain process.

On the whole, the elevated temperature favors the formation of phenylbisthiobarbiturate **3a**. *n*-PrOH appears to be the most suitable for the electrocatalytic process anion at cathode, which explains that reaction in propanol media proceeded with the highest yields. On the other hand, the longer reaction proceeds, the lower the current efficiency is, as the quantity of electricity passed increases.

This way a simple and effective method was found for electrolytic transformation of aromatic aldehydes and double excess of 1,3-diethyl-2-thiobarbituric acid (**2**) into 5,5'-(arylmethylene)bis(1,3-diethyl-2-thiobarbituric acids) in the electrolyzer without diaphragm. Under the optimal conditions (Table 1, entry 4), the electrolysis of aldehydes **1a–l** and 2 equiv of 1,3-diethyl-2-thiobarbituric acid (**2**) led to 5,5'-(arylmethylene)bis(1,3-diethyl-2-thiobarbituric acids) **3a–l** in 87–98% yields (current efficiency 870–980%) (Scheme 1). After the end of the electrolytic cascade process, the solution was evaporated to volume of 4 ml. The product crystallized from the concentrated reaction mixture and was isolated by filtration and washed on filter with chilled EtOH–H_2O, 4:1. The structures of all new compounds **3b–d**,**f–i**,**k**,**l** were confirmed by ^{1}H, ^{13}C NMR and

Scheme 2. The mechanism of electrocatalytic reaction of aldehydes **1** with 2 equiv of 1,3-diethyl-2-thiobarbituric acid (**2**)

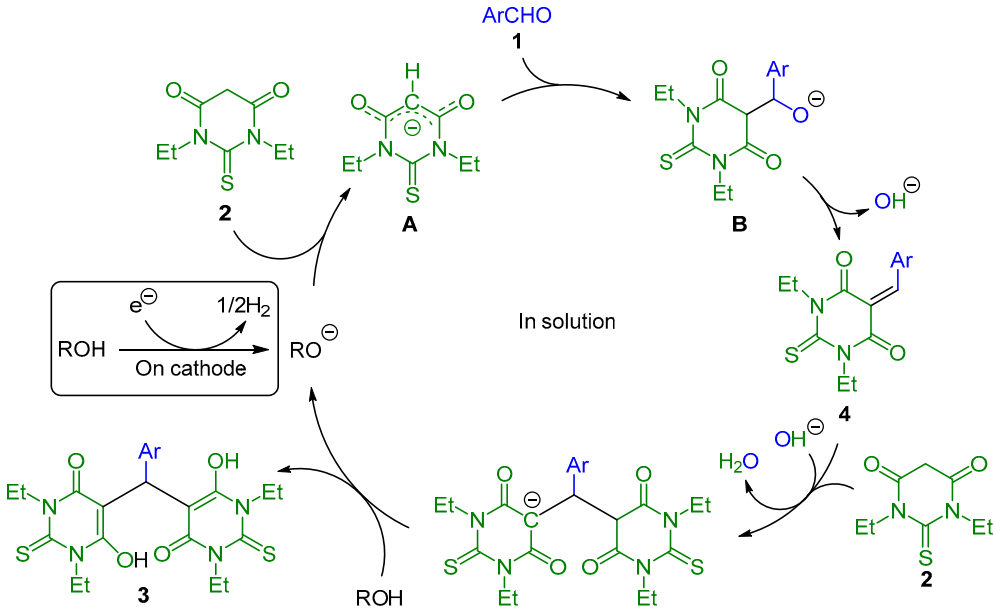

IR spectroscopy, mass spectrometry, and elemental analysis.

Earlier 5,5'-(arylmethylene)bis(1,3-diethyl-2-thiobarbituric acids) **3a**,**e**,**j** were obtained in 42–65% yields by the reaction of aldehydes **1a**,**e**,**j** with 4 equiv of 1,3-diethyl-2-thiobarbituric acid (**2**) in EtOH with reaction time of 8 h.[49] In comparison with the electrocatalytic method proposed above, this method uses a significant excess of 1,3-diethyl-2-thiobarbituric acid.

With the above-mentioned results and taking into consideration the mechanistic data on tandem Knoevenagel–Michael reactions,[50,51] the following mechanism for the electrocatalytic assembly of aldehydes with 2 equiv of 1,3-diethyl-2-thiobarbituric acid (**2**) forming 5,5'-(arylmethylene)bis(1,3-diethyl-2-thiobarbituric acids) **3a**–**l** was proposed (Scheme 2).

The first step of this electrochemically induced process is the deprotonation of alcoholic solvent at the cathode, which leads to the formation of an alkoxide anion. Then, interaction of the latter with 1,3-diethyl-2-thiobarbituric acid (**2**) results in the conjugate thiobarbiturate anion **A** formation (Scheme 2). The following process in the bulk of solution is reaction of anion **A** and aldehyde **1** with the elimination of a hydroxide anion and formation of Knoevenagel adduct **4**.[52] The hydroxide anion promoted Michael addition of the next molecule of 1,3-diethyl-2-thiobarbituric acid (**2**) to the electron-deficient Knoevenagel adduct **4** affords the end product of the electrocatalytic chain process, namely, substituted 5,5'-(arylmethylene)bis-(1,3-diethyl-2-thiobarbituric acid) **3** with the regeneration of the alkoxide anion as the last step of the catalytic cycle. Then, the catalytic chain process continues by the interaction of the alkoxide anion with the next molecule of 1,3-diethyl-2-thiobarbituric acid (**2**) (Scheme 2).

Molecular docking studies. Molecular docking has become a powerful approach for structure-based drug discovery, as docking programs are able to provide correct predictions.[53] Docking aims to predict a correct pose (binding mode) for a ligand in the binding pocket and to assess binding energy for those poses.

Catalases play important role in oxidation processes,[54] inflammation,[55] apoptosis,[56] and tumor stimulation.[57] Catalases take part in EtOH metabolism[58] and decrease voluntary EtOH consumption.[59] Therefore, we were prompted to carry out a docking study of the synthesized compounds **3a**–**l** and catalases and identify modes of their interaction.

To begin the investigation, the NAPDH binding site of beef liver catalase was chosen for docking studies, namely, structure 7CAT from the RCSB Protein Data Bank.[60] The protein structure was proposed by the CSD-CrossMiner software.[61] This software allows mapping a pharmacophore for a given structure. Unsubstituted compound **3a** was chosen for mapping as a reference structure. The most distant donors and acceptors of compound **3a** were selected (mapped) as pharmacophore features (Fig. 1*a*). To reduce the amount of results, ring fragment was mapped as well and Tanimoto index was selected as 0.9. The search was carried out in "pdb_crossminer" feature database.

As a result, three similar protein-ligand complexes from protein data bank were proposed: 7CAT (root-mean-square deviation of atomic positions (RMSD) 0.815), 5OYD[63] (RMSD 0.832), 6BF4[64] (RMSD 0.867). The structure 7CAT

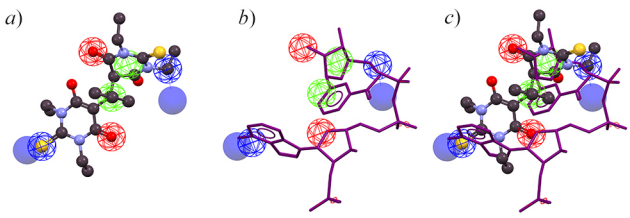

Figure 1. The pharmacophore of compound **3a**. *a*) The reference structure **3a**, *b*) the result of pharmacophore search – NADPH, *c*) the superposition of the reference and resulted structures. Blue mesh sphere represents a donor, translucent sphere is a donor projection, red sphere represents an acceptor, and green sphere represents a ring fragment.

was chosen as it had the lowest RMSD value. The conformation of NADPH in the binding site of beef liver catalase and its relation to pharmacophore are presented in Figure 1*b*, the superposition of reference compound **3a**, the pharmacophore, and NADPH are shown in Figure 1*c*.

The choices having been made, docking studies were carried out. The calculation process was performed with the Lead Finder tool in Flare software.[64] The protein structure was prepared with Buildmodel (a part of the Flare software). NADPH was used as a reference compound in docking studies. Several binding modes were calculated for each compound. Figure 2 shows that the first modes are the most favorable for each compound, and the results of the docking for the most favorable modes are presented in Table 2 (the rank score values for each compound are given in the Supplementary information file).

One should note that pharmacophore search with CSD-CrossMiner has provided a good target protein: the calculated binding energy (ΔG) is below –10 kcal/mol for compounds **3b**,**c**,**e**–**i**. The binding energy of compound **2g** (–11.25 kcal/mol) is almost twice as big as calculated energy for the reference compound NADPH (–5.91 kcal/mol).

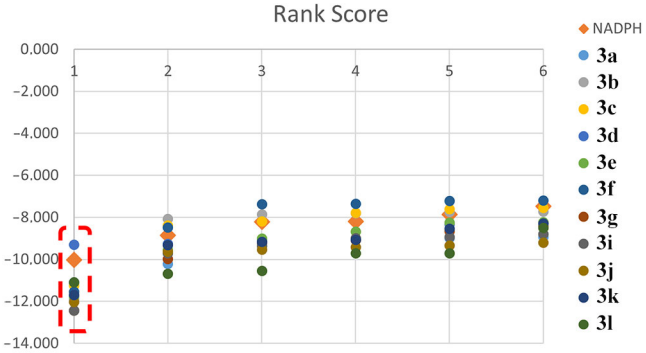

Figure 2. Ranking of binding modes to 7CAT. Six binding modes with rank score are given, rank score is dimensionless, the values for selected compounds are presented in Table 2.

Table 2. The results of the docking studies of compounds **3a**–**l** and NADPH to 7CAT or 1DGB*

Structures	7CAT		1DGB	
	ΔG,** kcal/mol	LE,*** kcal/mol·atom	ΔG, kcal/mol	LE, kcal/mol·atom
3a	–8.98	–0.27	–8.35	–0.25
3b	–10.80	–0.32	–9.20	–0.27
3c	–10.47	–0.28	–8.07	–0.22
3d	–8.63	–0.25	–8.15	–0.24
3e	–10.05	–0.29	–8.58	–0.25
3f	–10.00	–0.29	–8.25	–0.24
3g	–11.25	–0.33	–8.16	–0.24
3h	–10.20	–0.30	–9.31	–0.27
3i	–10.63	–0.29	–9.14	–0.25
3j	–9.71	–0.27	–8.84	–0.25
3k	–8.93	–0.27	–9.41	–0.29
3l	–8.15	–0.22	–7.06	–0.19
NADPH	–5.91	–0.12	–7.38	–0.15

* The data given for the best poses, the remaining data are given in the Supplementary information file.
** The energy of interaction between ligand and protein.
*** Ligand efficiency which is equal to ΔG per number of heavy (non-hydrogen) atoms in ligand molecule.

As it follows from distribution of binding energy (Fig. 3*a*), binding of compounds **3a**–**l** to 7CAT is even more beneficial than the binding of NADPH from thermodynamic point of view. The calculated binding values are broadly distributed, the binding energies for compounds **3a**–**l** are below –7÷–6 kcal/mol. In the 4th and 5th modes the difference in the energy between synthesized compounds and reference compound is the greatest: the best values for synthesized compounds are close to –10 kcal/mol, while the values for NADPH are above –4 kcal/mol.

Ligand efficiency (LE) of synthesized compounds is also beneficial due to the lower molecular mass and higher values of binding energies (see the Supplementary information file). The form of LE distribution is the same as binding energy distribution, and the values have the same tendency: the binding efficiency per atom of synthesized compounds **3a**–**l** is in the range of –0.3÷–0.2 kcal/mol·atom and the LE of NADPH is close to 0.1 kcal/mol·atom.

Compounds **3a**–**c**,**e**–**k** superimposed into binding pocket of 7CAT are demonstrated in Figure 4. The most favorable modes of compounds **3a**–**c** and **3e**–**k** are almost the same. In most cases, the aromatic fragment is exposed to hydrophobic surroundings or exposed to solvent.

Generally, the synthesized compounds and 7CAT form π–π stacking with Phe197. An atom of oxygen of barbituric fragment is tended to form hydrogen bond to Arg202, the adjacent atom of hydrogen is able to form bond to Tyr214 (compounds **3h**,**k**,**l**, and compounds **3c**,**d** through H_2O molecule), or Phe197 (compounds **3a**,**e**,**i**,**j**). Generally, barbituric fragments are exposed to positively charged or hydrophobic surroundings. Compound **3l** has slightly rotated position (counterclockwise, ~30°), while in the

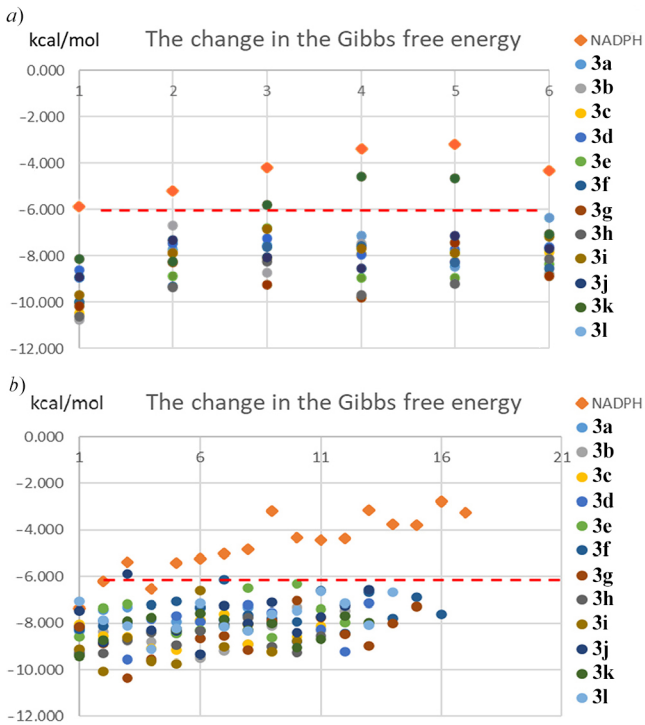

Figure 3. The distribution of binding energy of compounds **3a**–**l** to *a*) 7CAT and *b*) 1DGB. The horizontal axis line represents index of pose (binding mode). The calculated values for the first modes are given in Table 2.

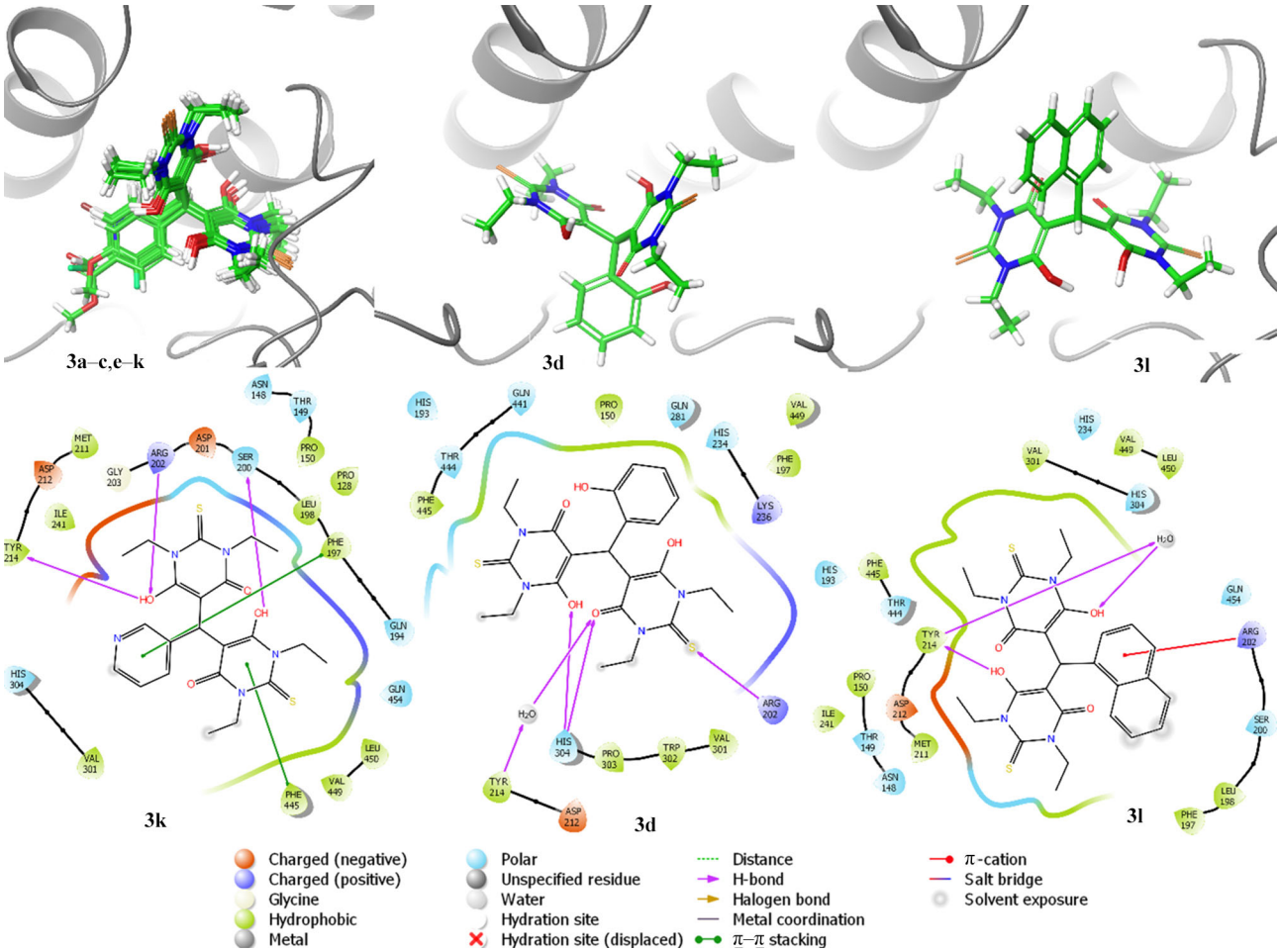

Figure 4. Position of docked compounds in binding pocket of 7CAT: superimposed compounds **3a**–**c**,**e**–**k**, compound **3d**, compound **3l**, and exemplary interactions of compounds **3k**,**d**,**l** inside the binding pocket.

position of compound **3d** the barbituric fragment and the aromatic fragment are interchanged (Fig. 4). Modes of compound **3d**,**l** are characterized by the lowest values of Gibbs free energy and ligand efficiency, but compound **3d** interacts with His304, while many compounds form interactions with Arg202, Phe197, and Tyr214 (Fig. 4). Compound **3d** forms hydrogen bond to Arg202, but **3l** forms a π–cation interaction. The aromatic fragment of compound **3d** is surrounded by hydrophobic chains, while aromatic fragment of compound **3l** is exposed to solvent. Barbituric fragments of compound **3d** are exposed to polar and positively charged surroundings, in contrast, barbituric fragments of compound **3l** are surrounded by hydrophobic and negatively charged surroundings (Fig. 4).

Encouraged by the results of docking compounds **3a**–**l** to 7CAT, we were prompted to investigate the relation of these compounds with human catalase. The structure 1DGB[54,65] of human erythrocyte catalase was selected for further investigation. The results of docking procedure are also presented in Table 2.

The distribution of binding energy has similar tendencies to the results mentioned above: the values of binding energy of synthesized compounds **3a**–**l** are below –6 kcal/mol, and the values of binding energy of NADPH are mostly above –6 kcal/mol (Fig. 3*b*). Nevertheless, the binding energy of the first mode of NADPH is –7.38 kcal/mol, and the values of binding energy below –9 kcal/mol are featured only by compounds **3b**,**h**,**i**,**k** (considering the first modes, Fig. 3*b*).

The LE follows the distribution of binding energy (Table 2) and due to the lower molecular mass and higher values of binding energies, the synthesized compounds have more beneficial LE distribution.

Best modes of compounds **3a**–**c**,**g**–**k** have similar positions in binding pocket of 1DGB. These compounds interact with Tyr215 and Arg203 (Fig. 5). Generally, aromatic fragments are surrounded by hydrophobic or positively charged chains, they are also exposed to solvent in case of compounds **3b**,**c**,**h**,**j**.

Best mode of compound **3e** has slightly rotated (counterclockwise ~30°C) and mirrored position (Fig. 5). Its aromatic fragment is exposed to polar and positively charged surroundings, while the barbituric fragment is surrounded by hydrophobic chains and slightly exposed to solvent. Compound **3e** has the most unusual mode and forms hydrogen bond with Trp303 and His305.

Interesting, that compounds **3f**,**l** have very close conformations to each other and similar surroundings, but different hydrogen bonding: compound **3l** forms π–cation interaction with Arg203 and there is an additional π–cation interaction with His305, while compound **3f** also forms a π–cation interaction with Arg203, and also forms the same

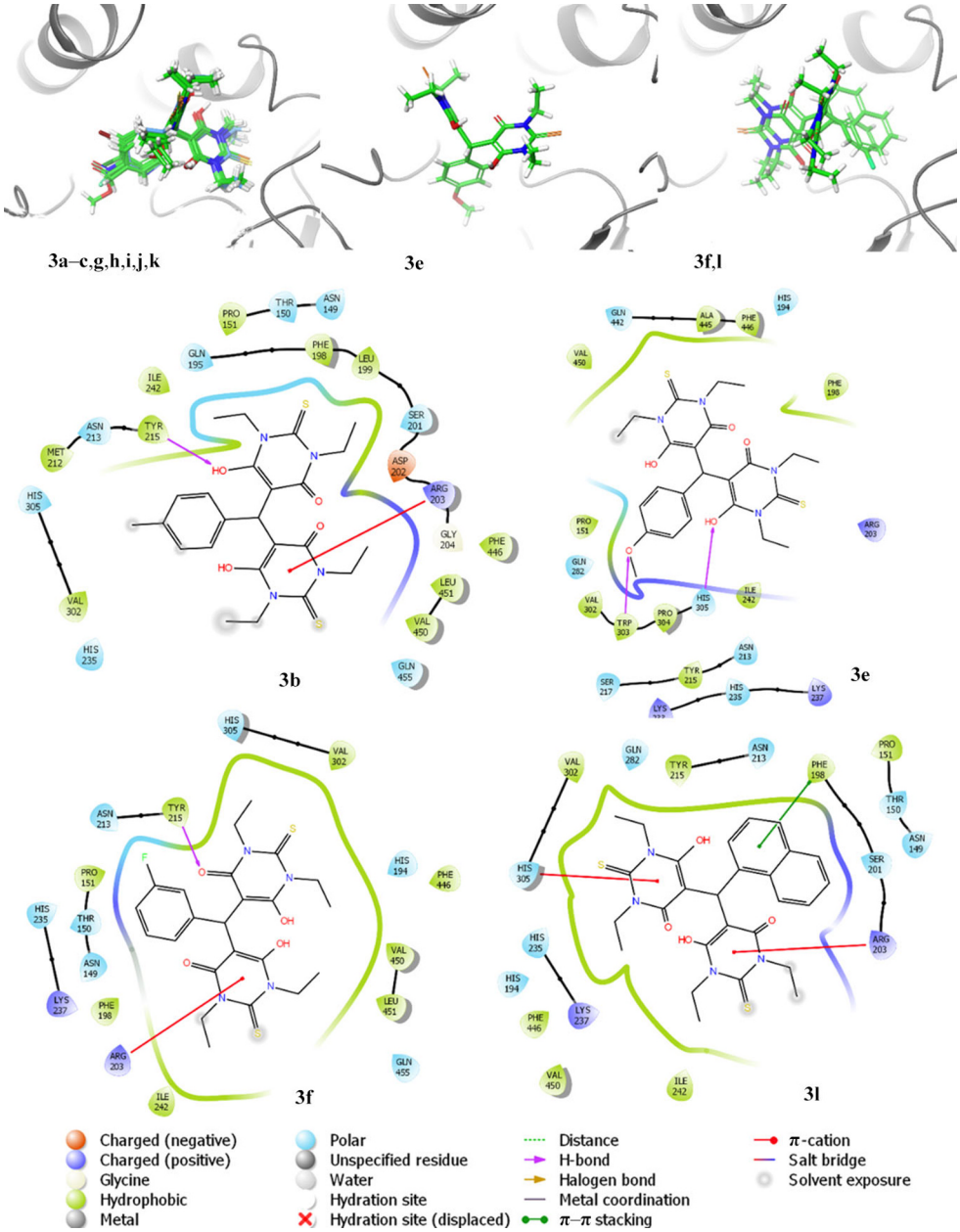

Figure 5. The position of synthesized compounds in binding site of 1DGB.

hydrogen bonds as compounds **3a**–**c**,**g**–**k**. At the same time, the position of compound **3l** is the least beneficial from thermodynamic point of view (binding energy is –7.06 kcal/mol, Table 2). Both compounds **3f**,**l** are surrounded by hydrophobic chains, but the aromatic fragments are among positively charged chains of 1DGB structure.

Thus, a new electrochemically induced fast and highly efficient reaction of aromatic aldehydes with 2 equiv of 1,3-diethyl-2-thiobarbituric acid in alcohols carried out in an undivided cell results in formation of the substituted 5,5'-(arylmethylene)bis(1,3-diethyl-2-thiobarbituric acids) in 87–98% yields and current efficiency of 870–980%. This new electrochemically induced tandem Knoevenagel–Michael process is simple, one-pot, and efficient approach to molecules containing two 1,3-diethyl-2-thiobarbituric acid fragments separated by *C*-aryl-substituted spacer, which are promising compounds for different biomedical applications, including anticonvulsant, antiAIDS agents, and anti-inflammatory remedies.

Instead of divided cells which are applied in many electroorganic syntheses, this efficient electrocatalytic procedure utilizes simple equipment, an undivided cell that is similar to common multineck flask. Commercially available, mostly stable starting compounds which need no preparation for the reaction, high yields of end compounds, simple procedures of synthesis and product isolation are also among the advantages of this method. Taking into consideration the short reaction time and tenfold current efficiency as well as low amount of waste, the proposed electrocatalytic method is promising as an environmentally benign scalable batch process.

The docking studies of synthesized compounds with some catalases were carried out. The investigations of proposed binding modes revealed the interactions with

different parts of NADPH binding site. The values of calculated binding energy and ligand efficiency of synthesized compounds are more beneficial than the calculated values for original ligand. Therefore, synthesized compounds are relevant for the further investigation of their activity as potent ligands of beef liver and human erythrocyte catalases.

Experimental

IR spectra were registered on a Bruker ALPHA-T FT-IR spectrometer in KBr pellets. ^{1}H and ^{13}C NMR spectra were recorded on Bruker Avance II-300 (300 and 75 MHz, respectively) and Bruker XWIND (500 and 126 MHz, respectively) spectrometers at ambient temperature with TMS as internal standard. Mass spectra (EI, 70 eV) were obtained directly with a Finningan MAT INCOS 50 spectrometer. For elemental analysis, PerkinElmer 2400 SERIES II and multi EA 5000 instruments were used. All melting points were measured with a Gallenkamp melting point apparatus and are uncorrected.

Synthesis of 5,5'-(arylmethylene)bis(1,3-diethyl-6-hydroxy-2-thioxo-2,3-dihydropyrimidin-4(1*H*)-ones) 3a–l (General method). A solution of aldehyde **1a–l** (5 mmol), 1,3-diethyl-2-thiobarbituric acid (**2**) (10 mmol), and NaBr (0.1 g, 1 mmol) in *n*-PrOH (20 ml) was electrolyzed in an undivided cell equipped with a magnetic stirrer, a graphite anode, and an iron cathode at 97°C under a constant current density of 5 mA/cm^2 (*I* 25 mA, electrode surface size 5 cm^2) until the catalytic quantity of 0.1 F/mol of electricity was passed (32 min). After the electrolysis was finished, the reaction mixture was concentrated to one fifth of its initial volume (ca. 4 ml) and cooled to 0°C to crystallize the solid product, which was then filtered off, twice rinsed with an ice-cold EtOH–H_2O, 4:1 mixture (4 ml), and dried under reduced pressure.

5,5'-(Phenylmethylene)bis(1,3-diethyl-6-hydroxy-2-thioxo-2,3-dihydropyrimidin-4(1*H*)-one) (3a). Yield 2.27 g (93%), white solid, mp 174–175°C (mp 174–176°C[49]).

5,5'-[(4-Methylphenyl)methylene]bis(1,3-diethyl-6-hydroxy-2-thioxo-2,3-dihydropyrimidin-4(1*H*)-one) (3b). Yield 2.57 g (96%), white solid, mp 164–166°C. IR spectrum, ν, cm^{-1}: 3435 (O–H), 2978, 2933, 2874 (C=S), 1620 (C=O), 1435 (C=C Ar), 1383, 1267, 1110, 786. ^{1}H NMR spectrum (300 MHz, $CDCl_3$), δ, ppm (*J*, Hz): 1.31 (6H, t, ^3J = 6.9, $2CH_3$); 1.39 (6H, t, ^3J = 6.9, $2CH_3$); 2.36 (3H, s, CH_3); 4.55–4.77 (8H, m, $4CH_2$); 5.65 (1H, s, CH); 6.88 (1H, br. s, OH); 7.02 (2H, d, ^3J = 7.7, H Ar); 7.14 (2H, d, ^3J = 7.7, H Ar); 13.85 (1H, br. s, OH). ^{13}C NMR spectrum (75 MHz, $CDCl_3$), δ, ppm: 12.0 (2C); 12.1 (2C); 21.0; 34.7; 44.6 (2C); 45.2 (2C); 97.6 (2C); 126.3 (2C); 129.2 (2C); 132.4; 136.4; 162.3 (2C); 163.8 (2C); 174.6 (2C). Mass spectrum, *m*/*z* (I_{rel}, %): 502 $[M]^+$ (38), 302 $[M–C_8H_{12}N_2O_2S]^+$ (83), 269 (82), 243 (13), 200 (53), 29 (100). Found, %: C 57.28; H 5.98; N 10.92; S 12.69. $C_{24}H_{30}N_4O_4S_2$. Calculated, %: C 57.35; H 6.02; N 11.15; S 12.76.

5,5'-{[4-(Trifluoromethyl)phenyl]methylene}bis(1,3-diethyl-6-hydroxy-2-thioxo-2,3-dihydropyrimidin-4(1*H*)-one) (3c). Yield 2.67 g (96%), white solid, mp 193–194°C. IR spectrum, ν, cm^{-1}: 3430 (O–H), 2987, 2938, 2878 (C=S), 1624 (C=O), 1438 (C=C Ar), 1379, 1266, 1111, 782. ^{1}H NMR spectrum (300 MHz, $CDCl_3$), δ, ppm (*J*, Hz): 1.32 (6H, t, ^3J = 6.9, $2CH_3$); 1.40 (6H, t, ^3J = 6.9, $2CH_3$); 4.53–4.75 (8H, m, $4CH_2$); 5.69 (1H, s, CH); 7.24–7.33 (2H, m, H Ar); 7.60 (2H, d, ^3J = 8.3, H Ar); 8.60 (1H, br. s, OH); 13.91 (1H, br. s, OH). ^{13}C NMR spectrum (126 MHz, $CDCl_3$), δ, ppm (*J*, Hz): 11.4 (2C); 11.5 (2C); 34.5; 44.1 (2C); 44.6 (2C); 96.3 (2C); 123.5 (q, $^1J_{CF}$ = 271.9; CF_3); 124.8 (q, $^3J_{CF}$ = 3.7, 2C); 126.2 (2C); 128.6 (q, $^2J_{CF}$ = 32.6, $\underline{C}CF_3$); 139.4; 161.7 (2C); 163.2 (2C); 174.0 (2C). Mass spectrum, *m*/*z* (I_{rel}, %): 556 $[M]^+$ (100), 356 $[M–C_8H_{11}N_2O_2S]^+$ (74), 323 (44), 200 (41). Found, %: C 51.65; H 4.82; F 10.11; N 10.01; S 11.38. $C_{24}H_{27}F_3N_4O_4S_2$. Calculated, %: C 51.79; H 4.89; F 10.24; N 10.07; S 11.52.

5,5'-[(2-Hydroxyphenyl)methylene]bis(1,3-diethyl-6-hydroxy-2-thioxo-2,3-dihydropyrimidin-4(1*H*)-one) (3d). Yield 2.26 g (87%), yellow solid, mp 141–143°C. IR spectrum, ν, cm^{-1}: 3376 (O–H), 2981, 2935 (C=S), 2526, 1631 (C=O), 1423 (C=C Ar), 1264, 1109, 896, 747. ^{1}H NMR spectrum (300 MHz, $CDCl_3$), δ, ppm (*J*, Hz): 1.25 –145 (12H, m, $4CH_3$); 4.51–4.76 (8H, m, $4CH_2$); 5.69 (1H, s, CH); 6.71 (1H, d, ^3J = 8.0, H Ar); 6.89–6.96 (1H, m, CH Ar); 7.07–7.21 (2H, m, CH Ar); 9.46 (3H, br. s, 3OH). ^{13}C NMR spectrum (75 MHz, $CDCl_3$), δ, ppm: 12.4 (2C); 12.5 (2C); 32.2; 44.6 (2C); 45.2 (2C); 98.3 (2C); 115.9; 120.6; 128.3; 128.8; 135.8; 153.8; 162.4 (2C); 163.1 (2C); 174.5 (2C). Mass spectrum, *m*/*z* (I_{rel}, %): 504 $[M]^+$ (4), 304 $[M–C_8H_{11}N_2O_2S]^+$ (83), 200 (69), 173 (87), 29 (100). Found, %: C 54.61; H 5.54; N 11.02; S 12.57. $C_{23}H_{28}N_4O_5S_2$. Calculated, %: C 54.74; H 5.59; N 11.10; S 12.71.

5,5'-[(4-Methoxyphenyl)methylene]bis(1,3-diethyl-6-hydroxy-2-thioxo-2,3-dihydropyrimidin-4(1*H*)-one) (3e). Yield 2.31 g, (89%), white solid, mp 135–137°C (mp 133–136°C[49]).

5,5'-[(3-Fluorophenyl)methylene]bis(1,3-diethyl-6-hydroxy-2-thioxo-2,3-dihydropyrimidin-4(1*H*)-one) (3f). Yield 2.41 g (95%), white solid, mp 196–197°C. IR spectrum, ν, cm^{-1}: 2981, 2935, 2876 (C=S), 2523, 1622 (C=O), 1424 (C=C Ar), 1380, 1266, 1108, 788. ^{1}H NMR spectrum (300 MHz, $CDCl_3$), δ, ppm (*J*, Hz): 1.32 (6H, t, ^3J = 6.9, $2CH_3$); 1.40 (6H, t, ^3J = 6.9, $2CH_3$); 4.55–4.77 (8H, m, $4CH_2$); 5.66 (1H, s, CH); 6.82–6.89 (3H, m, H Ar); 6.91–7.01 (1H, m, H Ar); 7.82 (1H, br. s, OH); 13.96 (1H, br. s, OH). ^{13}C NMR spectrum (75 MHz, $CDCl_3$), δ, ppm (*J*, Hz): 12.1 (4C); 34.9; 44.7 (2C); 45.2 (2C); 97.1 (2C); 113.8 (d, $^2J_{CF}$ = 23.9, C Ar); 113.9 (d, $^2J_{CF}$ = 23.9); 122.1 (d, $^4J_{CF}$ = 3.2); 129.9 (d, $^3J_{CF}$ = 8.4); 138.5 (d, $^3J_{CF}$ = 8.4); 162.3 (2C); 163.2 (d, $^1J_{CF}$ = 245.5); 163.8 (2C); 174.7 (2C). Mass spectrum, *m*/*z* (I_{rel}, %): 506 $[M]^+$ (18), 306 $[M–C_8H_{11}N_2O_2S]^+$ (35), 273 (27), 200 (39), 29 (100). Found, %: C 54.42; H 5.33; F 3.62; N 10.97; S 12.54. $C_{23}H_{27}FN_4O_4S_2$. Calculated, %: C 54.53; H 5.37; F 3.75; N 11.06; S 12.66.

5,5'-[(4-Chlorophenyl)methylene]bis(1,3-diethyl-6-hydroxy-2-thioxo-2,3-dihydropyrimidin-4(1*H*)-one) (3g). Yield 2.35 g (90%), white solid, mp 183–184°C. IR spectrum, ν, cm^{-1}: 3426 (O–H), 2977, 2932, 2874 (C=S), 1622 (C=O), 1438 (C=C Ar), 1383, 1268, 1109, 779. ^{1}H NMR spectrum (300 MHz, $CDCl_3$), δ, ppm (*J*, Hz): 1.31 (6H, t, ^3J = 7.0, $2CH_3$); 1.39 (6H, t, ^3J = 7.0, $2CH_3$); 4.54–4.77 (8H, m, $4CH_2$); 5.63 (1H, s, CH); 7.08 (2H, d, ^3J = 8.2, H Ar); 7.30 (2H, d, ^3J = 8.2, H Ar); 9.78 (1H, br. s, OH); 13.94 (1H, br. s, OH). ^{13}C NMR spectrum (75 MHz, $CDCl_3$), δ, ppm:

12.1 (4C); 34.7; 44.7 (2C); 45.2 (2C); 97.2 (2C); 127.9 (2C); 128.7 (2C); 132.7; 134.3; 162.3 (2C); 163.8 (2C); 174.7 (2C). Mass spectrum, *m/z* (I_{rel}, %): 524 $[M(^{37}Cl)]^+$ (38), 522 $[M(^{35}Cl)]^+$ (79), 324 $[M(^{37}Cl)–C_8H_{11}N_2O_2S]^+$ (54), 322 $[M(^{35}Cl)–C_8H_{11}N_2O_2S]^+$ (100), 289 (56), 200 (28). Found, %: C 52.73; H 5.23; Cl 6.65; N 10.59; S 12.13. $C_{23}H_{27}ClN_4O_4S_2$. Calculated, %: C 52.81; H 5.20; Cl 6.78; N 10.71; S 12.26.

5,5'-[(3-Bromophenyl)methylene]bis(1,3-diethyl-6-hydroxy-2-thioxo-2,3-dihydropyrimidin-4(1*H*)-one) (3h). Yield 2.61 g (92%), white solid, mp 198–200°C. IR spectrum, ν, cm^{-1}: 3427 (O–H), 3043, 2981 (C=S), 2523, 1620 (C=O), 1430 (C=C Ar), 1379, 1267, 1108, 781. ^{1}H NMR spectrum (300 MHz, $CDCl_3$), δ, ppm (*J*, Hz): 1.32 (6H, t, ^3J = 6.9, $2CH_3$); 1.40 (6H, t, ^3J = 6.9, $2CH_3$); 4.54–4.77 (8H, m, $4CH_2$); 5.64 (1H, s, CH); 7.09 (1H, d, ^3J = 7.8, H Ar); 7.22 (1H, dd, ^3J = 8.0, ^3J = 7.6, H Ar); 7.27 (1H, s, H Ar); 7.42 (1H, d, ^3J = 7.8, H Ar); 8.19 (1H, br. s, OH); 13.94 (1H, br. s, OH). ^{13}C NMR spectrum (75 MHz, $CDCl_3$), δ, ppm: 12.1 (4C); 34.8; 44.7 (2C); 45.3 (2C); 97.0 (2C); 122.8; 125.2; 129.7; 129.9; 130.0; 138.2; 162.3 (2C); 163.8 (2C); 174.7 (2C). Mass spectrum, *m/z* (I_{rel}, %): 568 $[M(^{81}Br)]^+$ (10), 566 $[M(^{79}Br)]^+$ (8), 368 $[M(^{81}Br)–C_8H_{11}N_2O_2S]^+$ (59), 366 $[M(^{79}Br)–C_8H_{11}N_2O_2S]^+$ (49), 335 (31), 333 (31), 200 (55), 29 (100). Found, %: C 48.54; H 4.77; Br 14.01; N 9.73; S 11.23. $C_{23}H_{27}BrN_4O_4S_2$. Calculated, %: C 48.68; H 4.80; Br 14.08; N 9.87; S 11.30.

Methyl 4-[bis(1,3-diethyl-6-hydroxy-4-oxo-2-thioxo-1,2,3,4-tetrahydropyrimidin-5-yl)methyl]benzoate (3i). Yield 2.57 g (94%), white solid, mp 195–197°C. IR spectrum, ν, cm^{-1}: 3443 (O–H), 2981, 2833 (C=S), 1717 (C=O), 1616, 1433 (C=C Ar), 1378, 1270, 1109, 779. ^{1}H NMR spectrum (300 MHz, $CDCl_3$), δ, ppm (*J*, Hz): 1.31 (6H, t, ^3J = 7.0, $2CH_3$); 1.40 (6H, t, ^3J = 7.0, $2CH_3$); 3.93 (3H, s, OCH_3); 4.53–4.77 (8H, m, $4CH_2$); 5.69 (1H, s, CH); 7.23 (2H, d, ^3J = 8.0, H Ar); 7.42 (2H, d, ^3J = 8.0, H Ar); 8.83 (1H, br. s, OH); 13.91 (1H, br. s, OH). ^{13}C NMR spectrum (75 MHz, $CDCl_3$), δ, ppm: 12.1 (4C); 35.3; 44.7 (2C); 45.3 (2C); 52.3; 97.2 (2C); 126.6 (2C); 128.9; 129.8 (2C); 141.3; 162.4 (2C); 163.8 (2C); 166.8; 174.7 (2C). Mass spectrum, *m/z* (I_{rel}, %): 546 $[M]^+$ (11), 346 $[M–C_8H_{11}N_2O_2S]^+$ (50), 313 (44), 200 (58), 29 (100). Found, %: C 54.86; H 5.46; N 10.20; S 11.61. $C_{25}H_{30}N_4O_6S_2$. Calculated, %: C 54.93; H 5.53; N 10.25; S 11.73.

5,5'-[(4-Nitrophenyl)methylene]bis(1,3-diethyl-6-hydroxy-2-thioxo-2,3-dihydropyrimidin-4(1*H*)-one) (3j). Yield 2.43 g (91%), white solid, mp 198–200°C (mp 198–199°C[49]).

5,5'-[(Pyridin-3-yl)methylene]bis(1,3-diethyl-6-hydroxy-2-thioxo-2,3-dihydropyrimidin-4(1*H*)-one) (3k). Yield 2.40 g (98%), white solid, mp 267–269°C. IR spectrum, ν, cm^{-1}: 3610, 3443 (O–H), 2975 (C=S), 1610 (C=O), 1432 (C=C Ar), 1382, 1270, 1108, 1013, 786. ^{1}H NMR spectrum (300 MHz, DMSO-d_6), δ, ppm (*J*, Hz): 1.17 (12H, t, ^3J = 6.9, $4CH_3$); 4.44 (8H, q, ^3J = 6.2, $4CH_2$); 6.43 (1H, s, CH); 7.93 (dd, ^3J = 8.1, ^3J = 5.7, 1H, CH Ar); 8.28 (1H, d, ^3J = 7.1, CH Ar); 8.58 (1H, s, H Ar); 8.69 (1H, d, ^3J = 5.7, H Ar); 9.05 (1H, br. s, OH); 16.98 (1H, br. s, OH). ^{13}C NMR spectrum (75 MHz, DMSO-d_6), δ, ppm: 12.2 (4C); 32.2; 43.0 (4C); 94.1 (2C); 126.6; 139.1; 140.0; 143.1; 144.6; 161.0 (4C); 174.6 (2C). Mass spectrum, *m/z* (I_{rel}, %): 489 $[M]^+$ (4), 289 $[M–C_8H_{11}N_2O_2S]^+$ (65), 256 (29), 200 (40), 29 (100). Found, %: C 53.85; H 5.53; N 14.18; S 13.01. $C_{22}H_{27}N_5O_4S_2$. Calculated, %: C 53.97; H 5.56; N 14.30; S 13.10.

5,5'-(1-Naphthylmethylene)bis(1,3-diethyl-6-hydroxy-2-thioxo-2,3-dihydropyrimidin-4(1*H*)-one) (3l). Yield 2.37 g (88%), white solid, mp 130–132°C. IR spectrum, ν, cm^{-1}: 3435 (O–H), 2980, 2934, 2874 (C=S), 1615 (C=O), 1428 (C=C Ar), 1381, 1267, 1109, 781. ^{1}H NMR spectrum (300 MHz, DMSO-d_6), δ, ppm (*J*, Hz): 1.21 (6H, t, ^3J = 6.9, $2CH_3$); 1.44 (6H, t, ^3J = 6.9, $2CH_3$); 4.54 (4H, q, ^3J = 6.5, $2CH_2$); 4.74 (4H, q, ^3J = 6.5, $2CH_2$); 6.21 (1H, s, CH); 6.44 (1H, br. s, OH); 7.32–7.51 (4H, m, H Ar); 7.55–7.61 (1H, m, H Ar); 7.82 (1H, d, ^3J = 7.9, H Ar); 7.88 (1H, d, ^3J = 7.9, H Ar); 13.89 (1H, br. s, OH). ^{13}C NMR spectrum (75 MHz, DMSO-d_6), δ, ppm: 11.9 (2C); 12.2 (2C); 34.0; 44.6 (2C); 45.3 (2C); 99.5 (2C); 122.8; 124.8; 125.5; 125.8 (2C); 126.1; 128.5; 129.5; 134.4; 154.8; 162.6 (2C); 163.3 (2C); 174.5 (2C). Mass spectrum, *m/z* (I_{rel}, %): 538 $[M]^+$ (7), 338 $[M^+–C_8H_{11}N_2O_2S]^+$ (100), 305 (50), 200 (36). Found, %: C 60.09; H 5.59; N 10.27; S 11.78. $C_{27}H_{30}N_4O_4S_2$: C 60.20; H 5.61; N 10.40; S 11.91.

Supplementary information file containing ^{1}H and ^{13}C NMR spectra for the new compounds and docking results is available at the journal website at http://link.springer.com/journal/10593.

The reported study was funded by the Russian Foundation for Basic Research (project 19-29-08013).

References

1. Cioc, R. C.; Ruijter, F.; Orru, R. V. A. *Green Chem.* **2014**, *16*, 2958.
2. Ho, T.-L. *Tandem Organic Reactions*; John Wiley & Sons: New York, 1992.
3. Anastas, P. T.; Warner, J. C. *Green Chemistry: Theory and Practice*; Oxford University Press: New York, 2000.
4. Moosavi-Zare, A. R.; Afshar-Hezarkhani, H.; Rezaei, M. M. *Polycyclic Aromat. Compd.* **2020**, *40*, 150.
5. Zeynizadeh, B.; Rahmani, S.; Ilkhanizadeh, S. *Polyhedron* **2019**, *168*, 48.
6. Liu, M.; Liu, C.-F.; Zhang, J.; Xu, Y.-J.; Dong, L. *Org. Chem. Front.* **2019**, *6*, 664.
7. Moosavi-Zare, A. R.; Goudarziafshar, H.; Jalilian, Z. *Prog. Chem. Biochem. Res.* **2019**, *2*, 59.
8. Maleki, R.; Koukabi, N.; Kolvari, E. *Appl. Organomet. Chem.* **2018**, *32*, e3905.
9. Elinson, M. N.; Sokolova, O. O.; Nasybullin, R. F. *Heterocycl. Commun.* **2015**, *21*, 97.
10. Khazaei, A.; Abbasi, F.; Moosavi-Zare, A. R. *New J. Chem.* **2014**, *38*, 5287.
11. Elinson, M. N.; Nasybullin, R. F.; Nikishin, G. I. *C. R. Chimie* **2013**, *16*, 789.
12. Moosavi-Zare, A. R.; Zolfigol, M. A.; Zarei, M.; Zare, A.; Khakyzadeh, V.; Hasaninejad, A. *Appl. Catal., A* **2013**, *467*, 61.
13. Safaei-Ghomi, J.; Khojastehbakht-Koopaei, B.; Zahedi, S. *Chem. Heterocycl. Compd.* **2015**, *51*, 34. [*Khim. Geterotsikl. Soedin.* **2015**, *51*, 34.]
14. *Organic Electrochemistry: Revised and Expanded*; Hammerich, O.; Speicer, B., Eds.; CRS Press: Boca Raton, 2016, 5th ed.
15. Yan, M.; Kawamata, Y.; Baran, P. S. *Angew. Chem., Int. Ed.* **2018**, *57*, 4149.
16. Nikishin, G. I.; Elinson, M. N.; Makhova, I. V. *Angew. Chem., Int. Ed.* **1988**, *27*, 1716.

17. Ogibin, Yu. N.; Elinson, M. N.; Nikishin, G. I. *Russ. Chem. Rev*. **2009**, *78*, 89. [*Usp. Khim.* **2009**, *78*, 99.]
18. Kashimura, S.; Matsumoto, K. In *Encyclopedia of Applied Electrochemistry*; Kreysa, G.; Ota, K.; Savinell, R. F., Eds; Springer: New York, 2014, p. 706.
19. Utley, J. H. P. *Top. Curr. Chem.* **1987**, *142*, 131.
20. Fotouhi, L.; Heravi, M. M.; Fatehi, A.; Bakhtiari, K. *Tetrahedron Lett.* **2007**, *48*, 5379.
21. Chiarotto, I.; Mattiello, L.; Feroci, M. *Acc. Chem. Res*. **2019**, *52*, 3297.
22. Elinson, M. N.; Feducovich, S. K.; Lizunova, T. L.; Nikishin, G. I. *Tetrahedron* **2000**, *56*, 3063.
23. Elinson, M. N.; Dorofeev, A. S.; Feducovich, S. K.; Gorbunov, S. V.; Nasybullin, R. F.; Miloserdov, F. M.; Nikishin, G. I. *Eur. J. Org. Chem.* **2006**, 4335.
24. Elinson, M. N.; Dorofeev, A. S.; Miloserdov, F. M.; Ilovaisky A. I.; Feducovich, S. K.; Belyakov, P. A.; Nikishin, G. I. *Adv. Synth. Catal.* **2008**, *350*, 591.
25. Elinson, M. N.; Vereshchagin, A. N.; Ryzhkov, F. V. *Chem. Rec.* **2016**, *16*, 1950.
26. Ilovaisky, A. I.; Merkulova, V. M.; Elinson, M. N.; Nikishin, G. I. *Russ. Chem. Rev.* **2012**, *81*, 381. [*Usp. Khim.* **2012**, *81*, 381.]
27. Elinson, M. N.; Vereshchagin, A. N.; Ryzhkov, F. V. *Curr. Org. Synth.* **2017**, *21*, 1427.
28. Arora, P.; Arora, V.; Lamba, H. S.; Wadhwa, D. *Int. J. Pharm. Res.* **2012**, *3*, 2947.
29. Taylor, A. P.; Robinson, R. P.; Fobian, Y. M.; Blakemore, D. C.; Jones, L. H.; Fadeyi, O. *Org. Biomol. Chem.* **2016**, *14*, 6611.
30. Johns, M. W. *Drugs* **1975**, *9*, 448.
31. Naguib, F. N. M.; Levesque, D. L.; Wang, E.-C.; Panzica. R. P.; El Kouni, M. H. *Biochem. Pharmacol.* **1993**, *46*, 1273.
32. Grams, F.; Brandstetter, H.; D'Alo, S.; Geppert, D.; Krell, H.-W.; Leinert, H.; Livi, V.; Menta, E.; Oliva, A.; Zimmermann, A. G. *Biol. Chem.* **2001**, *382*, 1277.
33. Maquoi, E.; Sounni, N. E.; Devy, L.; Olivier, F.; Frankenne, F.; Krell, H.-W.; Grams, F.; Foidart, J.-M.; Noël, A. *Clin. Cancer Res.* **2004**, *10*, 4038.
34. Fan, C.; Clay, M. D.; Deyholos, M. K.; Vederas, D. C. *Bioorg. Med. Chem.* **2010**, *18*, 2141.
35. Laxmi, S. V.; Reddy, Y. T.; Kuarm, B. S.; Reddy, P. N.; Crooks, P. A.; Rajitha, B. *Bioorg. Med. Chem. Lett.* **2011**, *21*, 4329.
36. Reddy, P. N.; Ponogoti, R. P.; Kasam, V.; Crooks, P. A. *Bioorg. Med. Chem. Lett.* **2013**, *23*, 1442.
37. Rayburn, E. R.; Ezell, S. J.; Zang R. *Mol. Cell Pharmacol*. **2009**, *1*, 29.
38. Marder, S. R.; Cheng, L.-T.; Tiemann, B. J.; Friedly, A. C.; Blanchard-Desce, M.; Perry, J. W.; Skindhøj, J. *Science* **1994**, *263*, 511.
39. Elinson, M. N.; Dorofeeva, E. O.; Vereshchagin, A. N.; Nasybullin, R. F.; Egorov, M. P. *Catal. Sci. Technol.* **2015**, *5*, 2384.
40. Elinson, M. N.; Dorofeeva, E. O.; Vereshchagin, A. N.; Nikishin, G. I. *Russ. Chem. Rev.* **2015**, *84*, 485. [*Usp. Khim.* **2015**, *84*, 485.]
41. Elinson, M. N.; Merkulova, V. M.; Ilovaisky, A. I.; Chizhov, A. O.; Barba, F.; Batanero, B. *J. Electrochem. Soc*. **2014**, *161*, G48.
42. Vereshchagin, A. N.; Elinson, M. N.; Dorofeeva, E. O.; Stepanov, N. O.; Zaimovskaya, T. A.; Nikishin, G. I. *Tetrahedron* **2013**, *69*, 1945.
43. Elinson, M. N.; Merkulova, V. M.; Ilovaisky, A. I.; Barba, F.; Batanero, B. *Electrochim. Acta* **2011**, *56*, 8219.
44. Elinson, M. N.; Feducovich, S. K.; Bushuev, S. G.; Zakharenkov, A. A.; Pashchenko, D. V.; Nikishin, G. I. *Mendeleev Commun*. **1998**, *8*, 15.
45. Wender, P. A. *Nat. Prod. Rep*. **2014**, *31*, 433.
46. Zang, W.; Yi, W.-B. *Pot*, *Atom*, *and Step Economy (PASE) Synthesis*; Springer: Cham, 2019.
47. Vereshchagin, A. N.; Elinson, M. N.; Zaimovskaya, T. A.; Nikishin, G. I. *Tetrahedron* **2008**, *64*, 9766.
48. Elinson, M. N.; Merkulova, V. M.; Ilovaisky, A. I.; Demchuk, D. V.; Belyakov, P. A.; Nikishin, G. I. *Mol. Diversity* **2010**, *14*, 833.
49. Adamson, J.; Coe, B. J.; Grassam, H. L.; Jeffery, J. C.; Coles, S. J.; Hursthouse, M. B. *J. Chem. Soc*., *Perkin Trans. 1* **1999**, 2483.
50. Elinson, M. N.; Dorofeev, A. S.; Nasybullin, R. F.; Feducovich, S. K.; Nikishin, G. I. *Electrochim. Acta* **2008**, *53*, 5033.
51. Elinson, M. N.; Dorofeev, A. S.; Nasybullin, R. F.; Nikishin, G. I. *Synthesis* **2008**, 1933.
52. Patai, S.; Israeli, Y. *J. Chem. Soc*. **1960**, 2025.
53. Torres, P. H. M.; Sodero, A. C. R.; Jofily, P.; Silva-Jr, F. P. *Int. J. Mol. Sci.* **2019**, *20*, 4574.
54. Putnam, C. D.; Arvai, A. S.; Bourne, Y.; Tainer, J. A. *J. Mol. Biol.* **2000**, *296*, 295.
55. Halliwell, B.; Gutteridge, J. M. C. *Biochem. J.* **1984**, *219*, 1.
56. Yabuki, M.; Kariya, S.; Ishisaka, R.; Yasuda, T.; Yoshioka. T.; Horton, A. A.; Utsumi, K. *Free Radical. Biol. Med.* **1999**, *26*, 325.
57. Miyamoto, T.; Hayashi, M.; Takeuchi, A.; Okamoto, T.; Kawashima, S.; Takii, T.; Hayashi, H.; Onozaki, K. *J. Biochem.* **1996**, *120*, 725.
58. Zimatkin, S. M.; Liopo, A. V.; Deitrich, R. A. *Alcohol.*: *Clin. Exp. Res*. **1998**, *22*, 1623.
59. Aragon, C. M. G.; Amit, Z. *Neuropharmacology* **1992**, *31*, 709.
60. (a) Murthy, M. R. N.; Reid, T. J., III; Sicignano, A.; Tanaka, N.; Fita, I.; Rossmann, M. G. PDB ID: 7CAT. DOI: 10.2210/pdb7CAT/pdb. (b) Fita, I.; Rossman, M. G. *Proc. Natl. Acad. Sci. U. S. A.* **1985**, *82*, 1604.
61. *CSD-CrossMiner 1.4.1*. Cambridge Crystallographic Data Centre. https://www.ccdc.cam.ac.uk/whitepapers/csd-crossminer-versatile-pharmacophore-query-tool-successful-modern-drug-discovery/. Accessed July 22, 2020.
62. (a) Attia, M. A.; Nelson, C. E.; Offen, W. A.; Jain, N.; Davies, G. J.; Gardner, J. G.; Brumer, H. PDB ID: 5OYD. https://doi.org/10.2210/pdb5OYD/pdb. (b) Attia, M. A.; Nelson, C. E.; Offen, W. A.; Jain, N.; Davies, G. J.; Gardner, J. G.; Brumer, H. *Biotechnol. Biofuels* **2018**, *11*, 45.
63. (a) Zhou, T.; Kwong, P. D.; PDB ID: 6BF4. https://doi.org/10.2210/pdb6BF4/pdb. (b) Zhou, T.; Zheng, A.; Baxa, U.; Chuang, G.-Y.; Georgiev, I. S.; Kong, R.; O'Dell, S.; Shahzad-Ul-Hussan, S.; Shen, C.-H.; Tsybovsky, Y.; Bailer, R. T.; Gift, S. K.; Louder, M. K.; McKee, K.; Rawi, R.; Stevenson, C. H.; Stewart-Jones, G. B. E.; Taft, J. D.; Waltari, E.; Yang, Y.; Zhang, B.; Shivatare, S. S.; Shivatare, V. S.; Lee, C. D.; Wu, C.-Y.; Mullikin, J. C.; Bewley, C. A.; Burton, D. R.; Polonis, V. R.; Shapiro, L.; Wong, C. H.; Mascola, J. R.; Kwong, P. D.; Wu, X. *Immunity* **2018**, *48*, 500.
64. (a) *Flare*, *3.0.0*, Cresset Software: Litlington, 2019. http://www.cresset-group.com/flare/. Accessed July 22, 2020. (b) Cheeseright, T.; Mackey, M.; Rose, S.; Vinter, A. *J. Chem. Inf. Model.* **2006**, *46*, 665. (c) Bauer, M. R.; Mackey, M. D. *J. Med. Chem*. **2006**, *62*, 3036. (d) Kuhn, M.; Firth-Clark, S.; Tosco, P.; Mey, A. S. J. S.; Mackey, M.; Michel, J. *J. Chem. Inf. Model* **2020**, *60*, 3120.
65. Putnam, C. D.; Arvai, A. S.; Bourne, Y.; Tainer, J. A. PDB ID: 1DGB. https://doi.org/10.2210/pdb1DGB/pdb.